

HAZROAD - MONITORING SYSTEM FOR HAZARD PREVENTION IN HIGHWAYS - A CASE STUDY IN BRAZILIAN FEDERAL HIGHWAYS

FERNANDA OLIVEIRA DE SOUSA

Department of Civil Engineering, Federal University of Rio de Janeiro, Brazil

fernandasousa@poli.ufrj.br

ABSTRACT

This study introduces a combination of Remote Sensing (RS) and Artificial Intelligence (AI) techniques to create a system for mapping and monitoring hazard events on Brazilian Federal highways. The proposed method is subdivided into four steps: I – Creating a Hazard inventory, II – Mapping hazards, III – Prediction of new events, and IV – Creating a web application for data management. The inventory was made using publications gathered from the official Twitter accounts of the Brazilian Federal Highway Police (PRF) and the National Department of Transportation Infrastructure (DNIT), agencies responsible for supervising and coordinating the Brazilian road system. The collected data were analyzed by Natural Language Processing (NLP) techniques and classified into two categories, Relevant and Irrelevant. The first is for cases where the text gave information about natural disasters on highways, and the second one is where the publication referred to other subjects. Three different models were employed for NLP classification, Logistic Regression (LogR), Random Forest (RF), and Support Vector Machine (SVM). They all provided a reasonable metrics score of approximately 97% using the Term Frequency-Inverse Document Frequency (TF-IDF) algorithm. In the following phases, both mapping and forecasting models were designed to emphasize geotechnical and flood disasters triggered by rainfall, the most common events in Brazil. To map flood extent and landslide, high-resolution satellite imagery acquired by the Sentinel Synthetic Aperture Radar (SAR), were used. The processing of these images allows the automatic calculation of the extent of flooding and landslide areas. In stage III, the forecast model was created by segmentation of the images collected in the preceding stage. The Deep Learning (DL) model U-NET was adopted for this purpose. The U-NET resulted in remarkable precision metrics ranges of 90%-96% for both cases. Moreover, hazard maps were obtained by a Multi-Criteria. Finally, the web app and database were built to report new events and store all the data from the previous phases.

1. INTRODUCTION

Brazil has the fourth most extensive road network in the world. Composed of 1,720,700.00 km of extension among urban and rural roads, of which 75,553.00 km are federal highways, the object of this study [1,2]. Figure 1 illustrates the Brazilian federal highway network. The figure shows in detail the Federal Highways in the state of Espírito Santo chosen as the study region of this paper. All federal highways in Brazil are given the prefix “BR-” and three digits, where the first one depends on their direction. They are classified into five categories: Radial, Longitudinal, Transversal, Diagonal, and Connecting. Radial (BR-0XX), are the highways that depart from the Federal Capital in the direction of the country’s extremes. Longitudinal (BR-1XX), are those that cross the country in a north-south direction. Transversal (BR-2XX) are the ones in the east-west direction. On the other hand, Diagonal (BR-3XX) can have two modes of orientation: Northwest-Southeast or Northwest-Southwest. And Connection highways (BR-4XX) are in either direction usually connecting at least one federal highway to international borders [1].

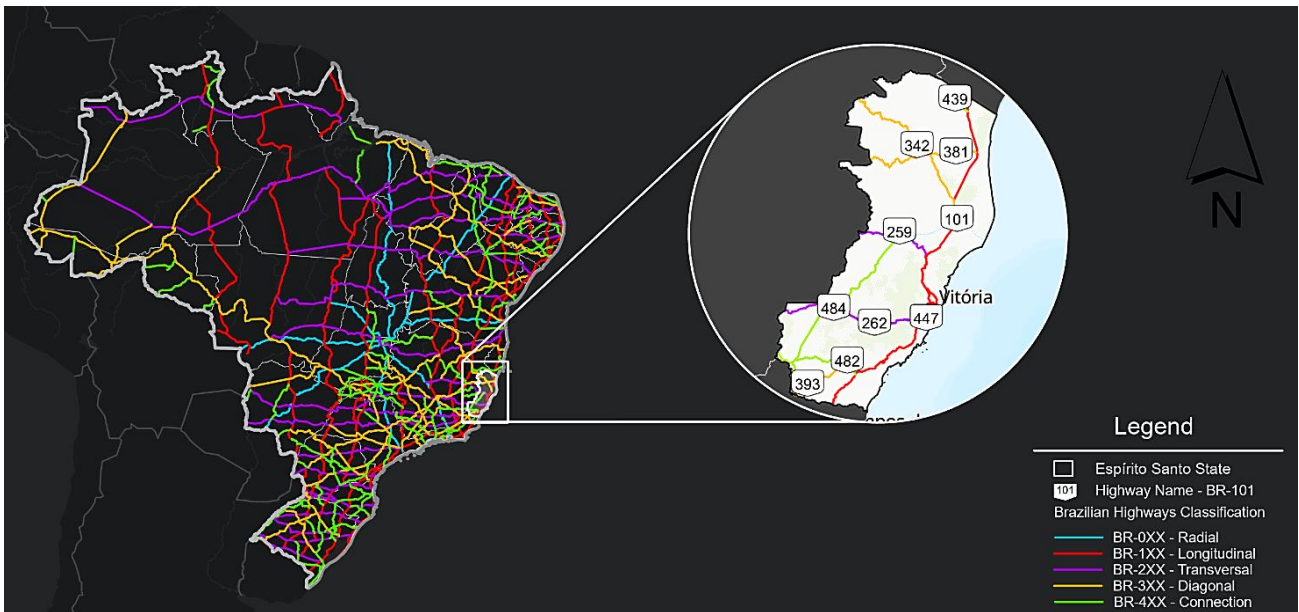


Figure 1 – Brazilian Federal Highways network

Brazilian transportation system is dependent mainly on road transportation, although it suffers from problems with infrastructure, safety, and longer travel times over long distances. In addition, factors such as the length of the network, the diverse hydro and geomorphologic conditions of the territory, and the insufficient investment in maintenance and repair have made them extremely vulnerable to weather events.

In several countries, floods, landslides, and rock falls in urban areas have become increasingly frequent due to climate changes. These events impact lives, the environment, economics as well the transportation system. In Brazil the overview is not different, to give a clear example, in December 2021, an intense volume of rainfall (4.5 times the historical average) was recorded, which resulted in landslides, floods, falling trees, and roadway destruction on several stretches of the BR 101, 174, 158, 358, and 459 highways. The disasters affected at least 116 municipalities, compromising the mobility of freight and passengers and consequently the country's economy. For the repair of the affected stretches, the Brazilian government has allocated about 39 million dollars through the MP 1086/2021 law proposal [3]. For this reason, the development of a disaster management plan for highways has become a requirement in Brazil. A disaster management plan consists of a set of strategies divided into four phases (i.e. Preparedness, Response, Recovery, and Mitigation) that are designed to create local networks and structures to cut down on the potential risks of disaster. In particular, the stage of preparedness social media and hazard maps play a fundamental role to prevent major damage. Social networks such as Twitter, Facebook, and Instagram have been fully implemented by stakeholders, public authorities, and humanitarian organizations to provide information about natural disasters, and broadcast risk alerts. Moreover, they can be considered an attractive tool to engage citizens in preparedness activities. Regarding the studies of risk areas, evacuation site destinations, and escape routes, hazard maps are used. They are based on geographic information that includes the history of previous disasters, as well as topographical and geological features that contribute to the land formation and disaster susceptibility in the area [4,5].

The combination of Remote Sensing and Artificial Intelligence has recently grown in the field of natural disaster management. In part, due to the improvement of geospatial technologies and the possibility to process high-resolution satellite imagery. But also because of the ascension of open data platforms such as Google Earth Engine (GEE) that allow access to geospatial Big data [6]. Cloud platforms facilitate the collection of high-resolution images

from pre-and post-natural disasters. The analysis of texture information within these images is essential for change detection [7]. Liu et al., supports that data-driven models, based on a Machine Learning (ML) approach have achieved good performances in landslide prediction. Such models have also been used to understand the relationship between the occurrence itself and its predictors [8]. In addition, Deep Learning (DL) techniques have been widely used in flood management, as in many cases they overcome the accuracy limitations of numerical models traditionally employed [9,10]. In recent years, several studies have been developing to identify the potential factors of risk and the possible damage caused by natural disasters. For the same purpose, this study was created to complement the existing references, highlighting the Brazilian case.

2. MATERIALS AND METHODS

In the HazRoad model, the inventory is developed by a combination of scraping data from information posted on Twitter and pre-processing natural language text. This allows for rapid database creation as well as near-real-time data input. Once past events have been known, the next step is to estimate affected areas by analyzing pre-and post-event images. Then, the hazard maps are designed. Subsequently, by employing deep learning techniques on these mapped regions, future events can be predicted. Finally, a rule-based approach is used to estimate the possibility of a hazard occurring throughout the region of interest. Specifically, the proposed framework consists of 14 successive steps. As illustrated in the following figure (Figure 2).

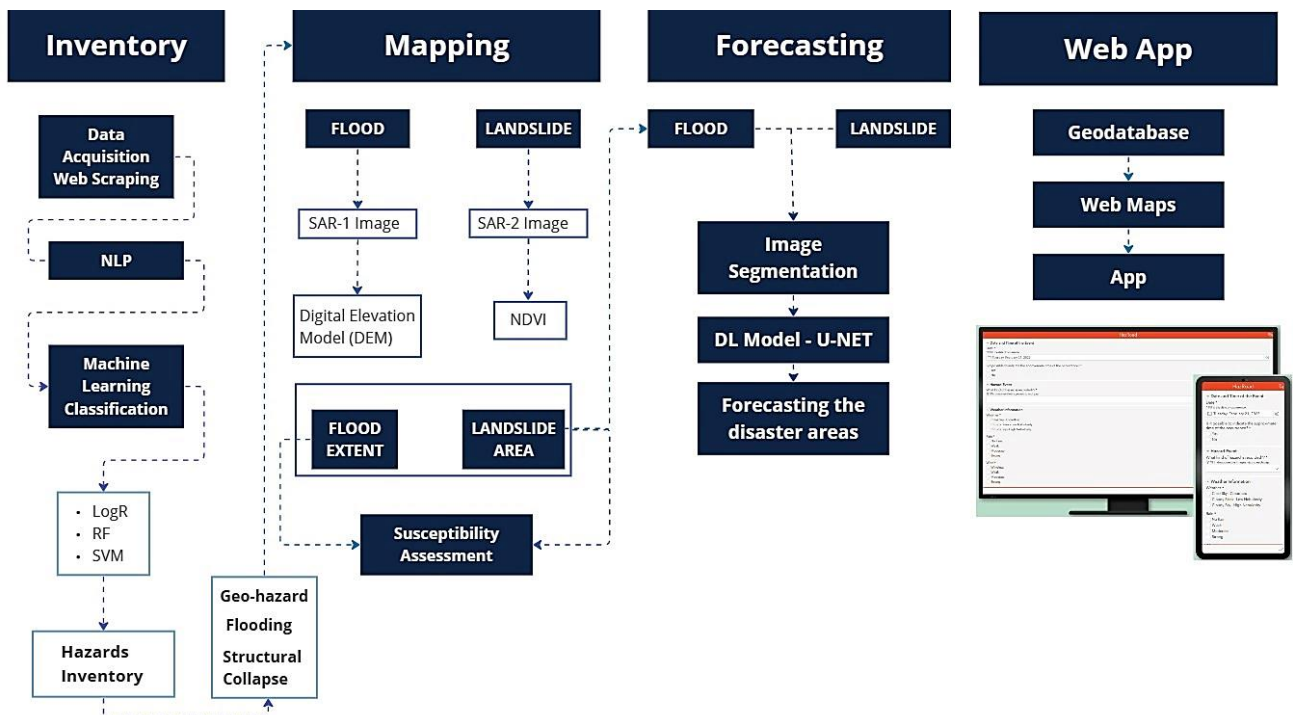


Figure 2 – Flowchart of HazRoad Model

The overall data acquisition and processing approaches, likewise the machine learning and remote sensing methods adopted to prepare this research will be described in the next sections.

2.1. Inventory of Historical Events

In Brazil, both disaster management and monitoring are coordinated by the National Civil Defense System of the municipalities in cooperation with the National Center for Monitoring

and Alerting Natural Disasters (CEMADEN) [11]. Nevertheless, there is not a specific sector that monitors natural disasters on highways or a survey of this data. Incidents such as inundations, landslides, or rock falls that occur on roads are usually published on the Twitter accounts of DNIT, and also of the Federal Highway Police of each state. Therefore, obtaining information on these events is technically challenging due to the lack of an official source. In fact, there are several possibilities to gather information from the Internet. Web Scraping is one of the most widely used to retrieve web data, for this reason, it was adopted in this study.

Natural language Processing was used before machine learning classification to filter and extract valuable information from tweets. NLP is defined as a subfield of Artificial Intelligence. Its main objective is the implementation of mechanisms, theories, elements, and systems that enable human-machine interaction using its own natural language [12]. HazRoad NLP pipeline consists of three main parts: pre-processing text, classification, and feature extraction. The pre-processing text means to clean data by removing noise, such as punctuation marks, additional spaces, and unnecessary character encodings (e.g. emoticons or emojis) [13]. In the classification phase, to establish whether the tweet reports a hazard or not, three different ML classification methods were applied, Support Vector Machines, Logistic Regression, and Random Forest. Finally, for feature extraction was employed the Term Frequency-Inverse Document Frequency approach. The process of feature extraction essentially consists of capturing important phrases and words contained in a text. TF-IDF is a method of feature extraction by performing a clustering process based on calculating the frequency of each word in the dataset used. [14]. The last stage aims to create a database with key information such as location, road name, and type of hazard.

2.2. Machine and Deep Learning Models

Both Deep Learning and Machine Learning are fields of Artificial Intelligence. Machine learning is the branch of computer science that provides computers the capability to learn without being explicitly programmed [15]. The ML mathematical models make predictions in tagged data through statistics theories [16]. Hence, it is generally necessary for some pre-processing to organize the data. On the other hand, Deep Learning excludes a significant amount of pre-processing steps required by machine learning. These algorithms can assimilate and process unstructured data, such as text and images, and they can also automate feature extraction, reducing reliance on human experts. DL is best suited for complex problems such as image recognition, speech recognition, and natural language processing [17]. AI models may be divided into three main classes: Supervised, Unsupervised and Reinforced Learning. The whole models used to develop this project are classified as supervised. This implies that labeled data sets were used to train the algorithms. For all models, the fitted data was split into training, test, and validation in a ratio of 70%, 20%, and 10%, respectively. The following is a brief description of the techniques employed in this study:

- **Logistic Regression:** Logistic regression is a linear model, analogous to linear regression. It finds a linear relationship between the variable target (dependent) and the characteristics of the variables (independent). In terms of the linear function, the logistic regression model predicts the probability $p(x)$ that the dependent variable belongs to the class of interest [18].
- **Random Forest:** RF is a supervised learning algorithm that is assumed to be versatile owing to its capacity to perform classification and regression tasks. When used, the algorithm produces a combination of decision trees to achieve a more precise prediction. This algorithm is used commonly because it is simple,

understandable, and presents good results in different types of machine learning analysis [19].

- **Support Vector Machine:** SVM Classifier is a supervised machine learning technique that employs hyperplanes to transform the nonlinear features into linear ones to classify features. A hyperplane is a decision plane that attempts to divide a set of objects and classify them [20].
- **U-NET:** U-Net network is a deep convolutional network that has widely been used in medical image segmentation [21]. Its major advantage is that it can be trained with a small amount of data. U-Net is a two-stage deep learning model. Its architecture includes an encoder model followed by a decoder model as depicted in figure 3.

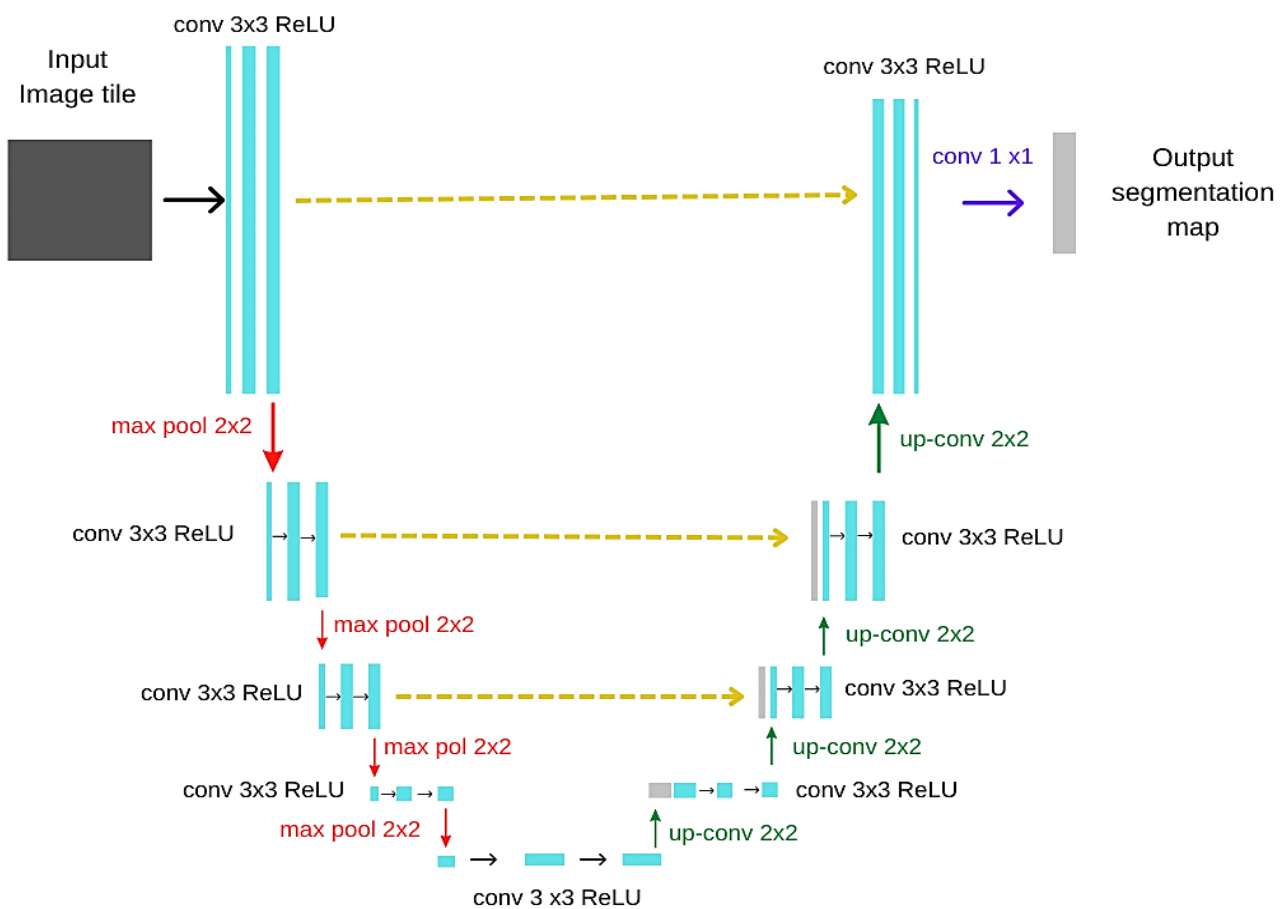


Figure 3 – U-Net Architecture

The encoding path is analogous to a typical CNN structure and consists of sequential convolution blocks. Every convolutional block contains two layers with a 3×3 kernel size and a 2×2 max-pooling layer. Each convolutional layer is triggered by the rectified linear unit (ReLU) activation function. In order to do non-linear down-sampling, a 2×2 max-pooling layer is added to the end of the convolutional block in the encoder path. In contrast, a 2×2 up-sampling layer is added to the decoder path. Following a 3×3 convolutional layer comes the up-sampling layer (see figure 2). This combination is what we refer to as learnable up convolution. At the final, a 1×1 layer constructs a binary mask. This model uses a set of input landslides and flooding images and their corresponding binary masks. During training and based on the binary mask as the target output, the model learns how to classify each pixel of the images into different object labels [21,22,23].

2.3. Performance Metrics

To evaluate the performance of all the models were used four metrics: Accuracy, F1 score, Precision, and Recall. Statistical metrics were computed based on true positive (TP), true negative (TN), false positive (FP), and false negative (FN) variables. All metrics and variables are briefly explained in table 1.

Table 1 – Performance Metrics

Metrics	Formula	Description
FP	False Positive	Number of actual negative samples classified as positive
FN	False Negative	Number of actual positive samples classified as negative
TP	True Positive	Number of actual positive samples correctly classified.
TN	True Negative	Number of actual negative samples correctly classified.
Accuracy	$\frac{TP + TN}{TP + TN + FP + FN}$	The ratio of samples that are correctly classified. This shows how well the model works.
F1 score	$\frac{2 \times Precision \times Recall}{Precision + Recall}$	It is a measure to evaluate classification systems and is a way to combine the precision and recall results
Precision	$\frac{TP}{TP + FP}$	The ratio of positive samples that are correctly classified. This indicates the good predictability of the model.
Recall	$\frac{TP}{TP + FN}$	The ratio of true positive samples that are correctly classified. This indicates the good predictability of the model.

2.4. Satellite Imagery Analysis

For each case of hazard detection, pre-and post-event images were used. In both cases, the time series scenes were acquired from the Google Earth Engine platform. For floods, Sentinel – 1 GRD-IW products are used. The Sentinel-1 mission consists of two polar-orbiting satellites (i.e. Sentinel-1A and Sentinel-1B) that work efficiently day and night, operating with a C-band synthetic aperture radar instrument that allows imagery acquisition regardless of weather or lighting conditions. It collects Synthetic Aperture Radar (SAR) data in single or dual polarization over 6 days. In order to simplify the handling of the images employed in this project, it was adopted the following pre-processing procedures [24]. The key aspects of pre-processing can be listed as follows:

1. **Apply Orbit File:** This operation enables the automatic download and update of orbit state vectors in product metadata for each SAR picture, providing more accurate satellite location and velocity information.
2. **Thermal Noise Removal:** Reduces noise effects in the inter-sub-swath texture, particularly by normalizing the backscatter signal across all Sentinel-1 imagery, decreasing the number of discontinuities among both sub-swaths for scenes acquired in multi-swath modes.
3. **Calibration:** Calibration is the method by which digital pixel values are converted to radiometrically calibrated SAR backscatter. The Sentinel-1 GRD product includes the information needed to apply the calibration equation.

4. **Speckle Noise removal:** Speckle filtering is a technique for improving image quality by minimizing speckles. It appears as a result of the interference of waves reflected from a large number of elementary scatterers.
5. **Terrain Correction:** The pixels are projected onto a map system and re-sampled to a spatial resolution of 10 m. Topographic corrections are also accomplished using a Shuttle Radar Topography Mission (SRTM) digital elevation model (DEM). It corrects the distortions in the terrain's areas.
6. **Conversion Linear into dB:** A logarithmic transformation is used to convert the unitless backscatter coefficient to dB.

Landslide identification differs from flood identification in terms of data acquisition and pre-processing. First, Sentinel-2 scenes were utilized in landslide cases. Furthermore, the pre-processing techniques used for Sentinel-2 products are less complex than the ones employed for flood detection (i.e. Sentinel – 1 scene). Its steps consist of filtering clouds and compositing all images selected. Both techniques are described below:

1. **Filter Clouds:** This implies that the less cloudy Sentinel-2 granules are selected by filtering the collection of images obtained during the pre-and post-event timeline. The process is based on the proportion of cloud cover. The cloud threshold of 30% was used in this study [25].
2. **Composite Images:** Pixel-based image compositing is a technique used in remote sensing to overcome some of the limitations such as data availability, cloud coverage, image archive discontinuity, atmospheric interference, and radiometric inconsistencies caused by seasonal differences or changes in sun angles [26,27]. The HazRoad algorithm calculates the normalized difference vegetation index (NDVI) to determine the composition of landslide areas. Scheip et al., proposed this compositing method in 2021, which is distinguished by the use of Google Earth Engine (GEE) to generate and perform calculations on a greenest-pixel composite. The greenest pixel composite is defined as the highest NDVI value calculated for the entire compilation of images, it means pre- and post-event scenes [28].

2.5. Hazard Mapping

According to a definition provided by The United Nations Office for Disaster Risk Reduction (UNDRR), a hazard is a process, phenomenon, or human activity that can result in death, injury, or other health consequences, property damage, economic and social interruption, or environmental degradation. This definition also subdivided hazard into three categories: Anthropogenic, Natural, and Socio-natural [29]. In this paper, the term 'hazard' will be used solely to refer to the natural category. Natural hazards are those associated mainly with natural processes and weather events. They include floods, volcanoes, earthquakes, tsunamis, and landslides.

Specifically, for the HazRoad model, a slightly different proposal was adopted. Natural disasters were grouped into three classes: Geohazards, Structural Collapses and Floods. The Geo-hazard category covers landslides, erosion, and rock falls. Solheim et al. [30], define geohazards as incidents generated by geological, geomorphological, or climatic conditions or processes that pose serious threats to human life, property, and the natural and built environment. Regarding, Structural Collapse the category includes road and bridge collapses, and potholes in the road. And flooding refers to instances of flash flooding along

the highway. This classification system is useful because it helps distinguish common occurrences on highways.

Overall, several conditioning factors can be considered for mapping hazards. For example, the Global Facility for Disaster Reduction and Recovery (GFDRR) [31] recommends that for mapping road disasters factors such as terrain, rainfall, road alignments, population data, land cover, and land use should be included. Antzoulatos et al. [32], support that the most relevant factors for flood mapping are elevation, slope, and aspect, all topographic parameters, which are extracted from digital elevation models (DEM) of the study area. The same conditioning factors were considered to design the HazRoad mapping models. For both, the elevation models were obtained using the Shuttle Radar Topography Mission (SRTM). The SRTM V3 (SRTM Plus) product provided by NASA JPL has 1 arc-second (approximately 30m) resolution [33,34].

2.6. Study Area

Due to the large extension of the Brazilian road network, and the availability of satellite images, it was chosen as the study area for the Remote Sensing and Deep Learning models (steps 2 and 3) only the regions with a higher frequency of floods and mass movements in the last three years. In particular, this work focuses on fourteen stretches of highway between the municipalities namely Serra, Cariacica, Viana, and Domingos Martins, all located in the state of Espírito Santo, as shown in Figure 4.

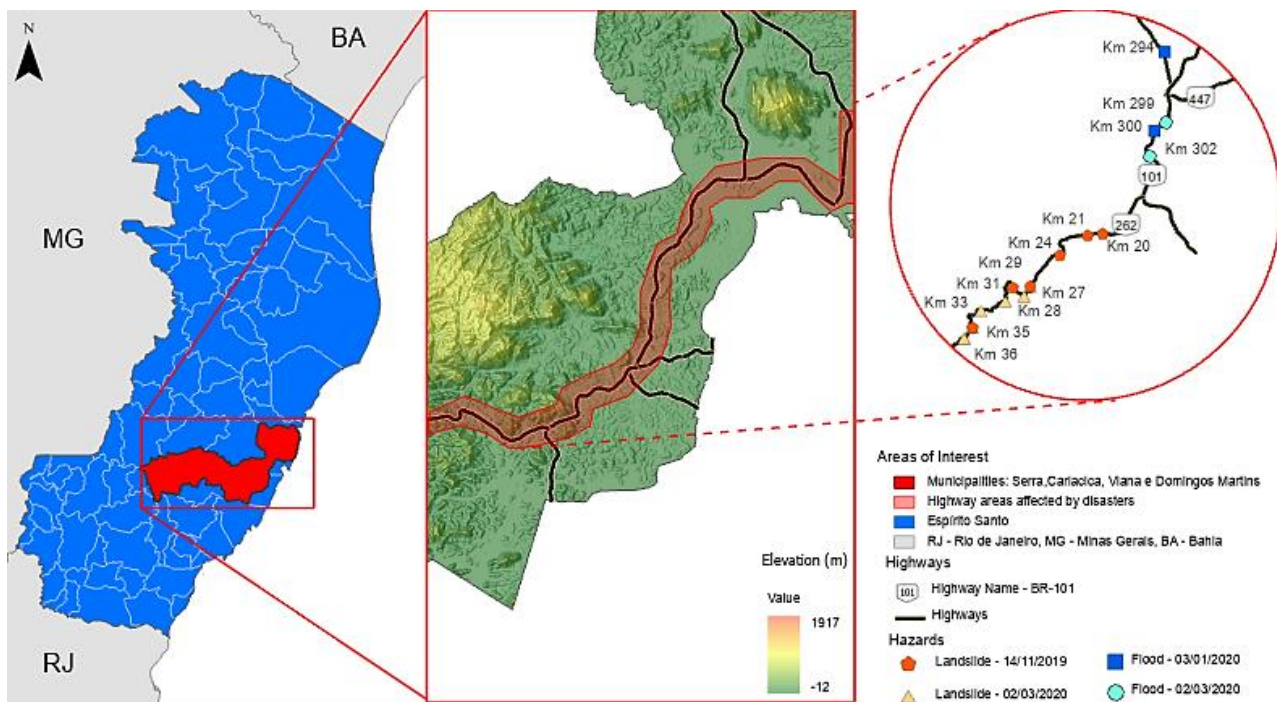


Figure 4 – Study area

Espírito Santo is located in the southeast region of Brazil. Covering an area of 46,095,583 km², it is the fourth smallest Brazilian state. Nevertheless, its geographical location turns it into an important link between the country's regions. It borders the states of Bahia (to the north), Minas Gerais (to the west), Rio de Janeiro (to the south), and the Atlantic Ocean (to the east). Its road network comprises ten Federal highways (see Figure 1), among them BR-101 and BR-262, which are the targets of this study. BR-101 is a longitudinal highway that crosses almost the entire Brazilian coast. BR-262 is a transverse highway that connects the coast to Minas Gerais and Mato Grosso do Sul. It serves as an important exit corridor for cattle, agriculture, and mining products.

The study domain is located in the central zone of Espírito Santo, which has a great variation in altitude. Regarding topography, the study area is characterized by the presence of low elevations in the municipality of Serra, where kilometers 294, 299, 300, and 302 of the BR-101 highway are located, and steep slopes in the sections of the BR-262 between Cariacica and Domingos Martins. From the geomorphological point of view, this area is divided into two morpho-structural groups, the Sedimentary Deposits, near the Serra, and the Remobilized Fold Bands in the other three municipalities. The sedimentary deposits are defined by the occurrence of sandy and sandy-clay sediments with gravel levels, basically from the Barrier Formation group and coastal environments, deposited during the Cenozoic period. While the remobilized fold belts are distinguished by evidence of crustal movements, with fault marks, block displacements, and transverse faulting, imposing clear structural control over the present morphology [35]. Regarding the hydrological aspects, the study area is comprised of two hydrographic basins, Santa Maria da Vitória River Basin (Serra and Cariacica), and Jucu River Basin (Domingos Martins, Cariacica, and Viana). According to data from the National Water Agency (ANA), the respective basins present high vulnerability and frequency to flood events. It is worth noting that the studied stretches in the Serra region are located in a fluvial accumulation zone, and therefore are subject to periodic flooding [36].

2.7. Mapping Areas Affected by Landslides and Floods

This step aims at outlining areas affected by mass movements or floods. For this, Sentinel satellite images were collected at different time intervals, before and after each event. Both the acquisition and processing of these images were performed on the Google Earth Engine platform. The mapping phase is crucial for the development of the project because the creation of the forecast model database depends on the images generated by it.

On November 14, 2019, an intense rainfall struck the mountainous region of the state of Espírito Santo, specifically between the municipalities of Viana and Domingos Martins. As a result, at least 6 points of landslides were registered on BR-262 that needed to be blocked. According to information from the transportation department, at least 77 points of landslides were reported on roads in this area between November 14 and 19 [37]. To map these events, 53 pre-and post-disaster satellite images from SAR-2 were collected. The definition of affected areas was achieved through a time series analysis of the Normalized Difference Vegetation Index (NDVI). In recent studies, the analysis of vegetation changes detected from abrupt NDVI declines in a short period has been employed for the rapid identification of landslides [38]. The methodology consists of calculating the difference between the NDVI from post-event of pre-event. The index is calculated by Equation 1. Then, it is defined as a data-driven threshold. In this study was applied the model proposed by Zhu and Woodcock [39] which measures the difference between observations and model predictions for each range/index, and the value found is normalized by three times the Root Mean Squared Error RMSE (Equation 2).

$$NDVI = \frac{NIR-Red}{NIR+Red} = \frac{B8 - B4}{B8 + B4} \quad (1)$$

Where:

NIR = light reflected in the near-infrared spectrum

Red = light reflected in the red range of the spectrum

B8 and B4 = Bands from Sentinel SAR-2, 10m resolution

$$\frac{1}{k} \sum_{i=1}^k \frac{|\rho(i,x) - \hat{\rho}(i,x)_{OLS}|}{3xRMSE_i} > 1 \quad (2)$$

Where:

x = Julian date

i = the i -th satellite band

$\rho(i, x)$ = observed value for the i -th satellite Band at Julian date x

$\hat{\rho}(i, x)$ = predicted value for the i -th satellite Band at Julian date x based on OLS fitting

Finally, landslide areas are defined as those have NDVI values greater than the threshold and slope value over 10%. Figure 5 illustrates the NDVI images from the study area pre- and post-event (Landslide, November 14, 2019).

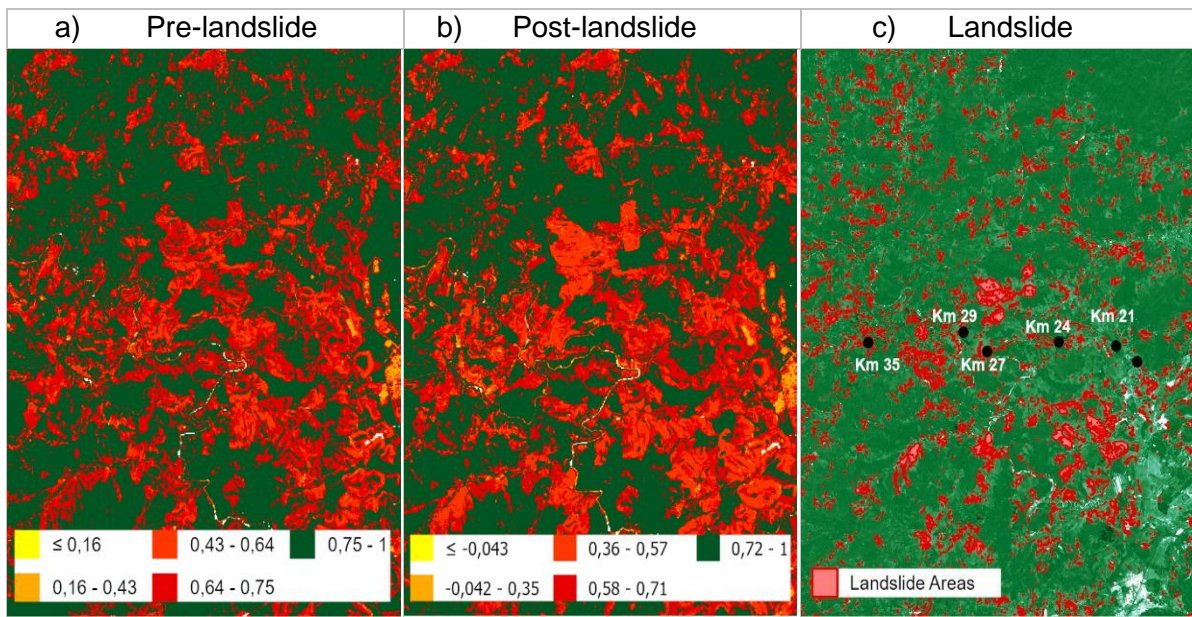


Figure 5 – NDVI values and Landslide areas

NDVI index ranges from -1.0 to 1.0, representing the variation of photosynthetic activity of the analyzed area. Negative values are formed mainly by water or snow, and values close to zero usually indicate bare rocks and soil. Values smaller than 0.1 correspond to bare areas of rocks, sand, or snow. Moderate values (from 0.2 to 0.3) represent shrubs and grasslands, while high values (from 0.6 to 0.8) indicate a higher density of green vegetation. [40,41].

For flood detection, 32 Sentinel-1 images were used. The SAR collection is Ground Range Detected High Resolution (GRDH) products with a resolution of 10 × 10 m. All data were acquired from the GEE platform in Interferometric Wide Swath (IW) mode in VH polarization. The image acquisition period ranges from December 1, 2019, to January 31, 2020.

The flooding event occurred on January 2 and 3, 2020, with a total rainfall accumulation of 491.83 mm in 48h in the municipalities of Cariacica, Viana, and Serra [42]. In Viana, the heavy rain flooded four sections of BR-262, near the access to the Marcílio de Noronha neighborhood. Visual representation of the SAR images is shown in Figure 6. The image processing steps were described in Section 2.4. The initial threshold calculation is performed by the difference between the images converted into dB after and before the event (Equation 3).

$$Threshold = \log (Post_{event} - Pre_{event}) \quad (3)$$

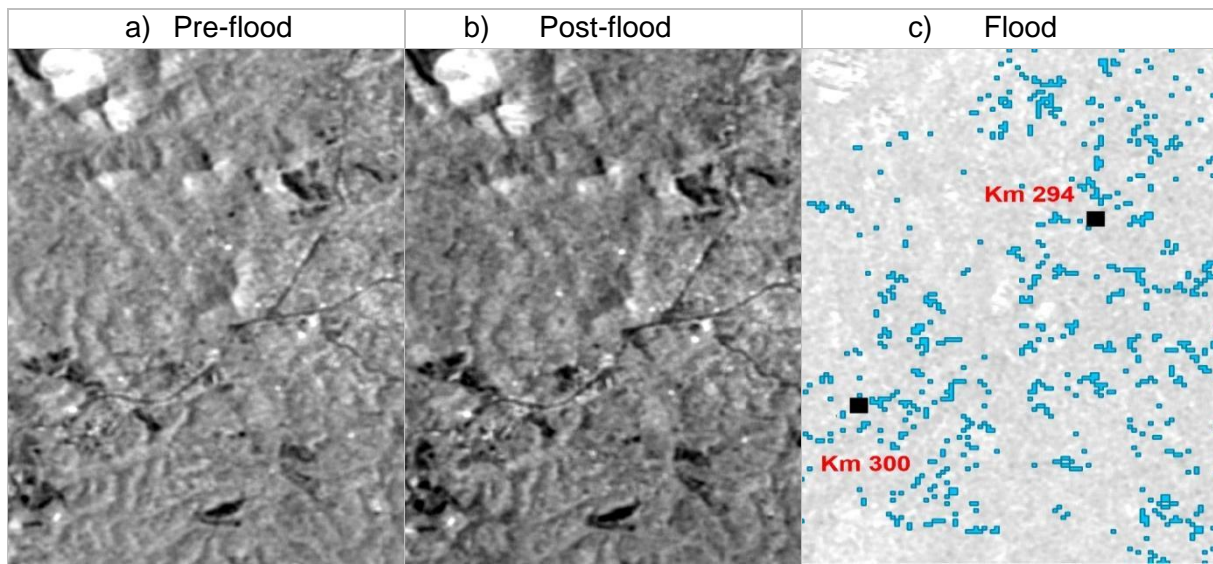


Figure 6 – Backscatter images pre-and post-event and Flooded areas

In order to increase the probability of estimating a correct threshold, it was decided to split the study area into 50 polygons and calculate the threshold for each of them. The final average threshold is the arithmetic mean of the obtained values. However, before delimiting the flooded areas, it is necessary to define the permanent water bodies such as rivers, streams, and lakes (water seasonality 10 months of the year). Then, a mask is created to differentiate the permanent water pixels from the flood pixels. Flooded areas are those where the set of pixels does not belong to the water bodies, has a slope less than or equal to 5%, and the difference between pre-and post-image is greater than the average threshold.

2.8. Hazard Assessment

In this study, hazard assessment is performed using Analytic Hierarchy Process (AHP). AHP is a semi-quantitative method Multi-Criteria Analysis (MCA) approach developed by Saaty in 1980 [43]. Its methodology consists of, splitting a complex problem into simple criteria, where the decisions are taken considering the weight of each criterion calculated in a pairwise comparison matrix [44]. This matrix is drawn based on the element comparison scale. The scale ranges from 1 to 9 where 1 is equal to “Equally important values” (Two factors contribute equally to the objective) and 9 equals extremely important values. On the other hand, the even numbers 2,4,6, and 8 are intermediate values (intermediate preference between adjacent scales). Each pair within each criterion is assigned a score. This score indicates how well option "A" satisfies criterion "B". The scores are then normalized and averaged. Ten criteria are applied to "judge" the relative importance of one indicator compared to another. The pairwise comparison tables were filled in for nine risk factors (e.g. slope, TWI, etc.) in the area of natural disasters. Their results were normalized and examined with the Consistency Ratio (CR) test represented in the equation below [45]. CR depends on the Randomness Index (RI) that is shown in Table 2.

$$CR = \frac{CI}{RI} = \frac{1}{RI} \left(\frac{\lambda - N}{N-1} \right) \quad (4)$$

Where:

CI = Consistency Index

RI = Random Index

λ = Major Eigen value

N = Criteria number

Table 2 – Random Index (RI) by Saaty (1980) [44]

N	1	2	3	4	5	6	7	8	9	10	11	12	13	14	15
RI	0.0	0.0	0.58	0.9	1.12	1.24	1.32	1.41	1.45	1.49	1.51	1.48	1.56	1.57	1.58

In HazRoad model, complex problems are defined as flood and landslide events. In addition, the criteria are defined based on causative factors to hazards. Several researches have considered slope, slope aspect, soil, elevation, land cover and use, drainage, distance from roads, distance from rivers, Topographic Wetness Index (TWI), and precipitation of the region as main causative factors of landslides and floods [46].

3. RESULTS AND DISCUSSION

Table 3 shows the summary of the performance metrics for the Natural Language Processing model.

Table 3 – Performance metrics for NLP models

Supervised Classifier	Accuracy	Precision	Recall	F1-Score
Logistic Regression	0.97	0.97	0.97	0.97
Support Vector Machine	0.97	0.97	0.97	0.97
Random Forest	0.97	0.96	0.97	0.96

The performance metrics for the HazRoad NLP framework present significant outcomes, all close to 1.0. Interestingly, these values for the three classifiers used were relatively equal. To distinguish which model is the best among the possibilities, the feature importance metric was adopted. Feature importance refers to techniques that assign a score to input features based on their usefulness in predicting a target variable. Their scores play an important role in a predictive modeling project, including providing information about the data. The classifier that presented the best results was the Logistic Regression, which was effective in identifying the following keywords as the most frequent terms: flood, hillside, landslide, erosion, collapse, road sinking, bridge collapse, and pothole.

Figure 7 provides the results obtained from the analysis of the tweets released by DNIT and the Federal Highway Police.

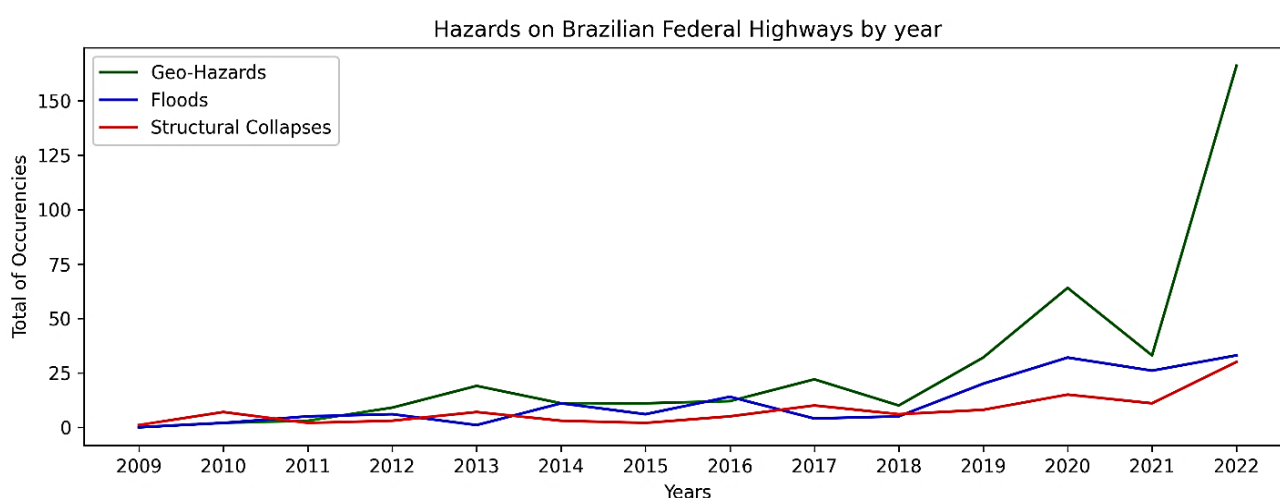


Figure 7 – Hazards recorded from tweets from 2009 to 2022

The graph shows the evolution of the number of disasters in the period between 2009 and 2022. From the chart, it is possible to observe a significant increase in events recorded from 2018. A possible explanation for this may be the increased accumulation of rainfall in the southern, southeastern, and northeastern regions of Brazil. These regions concentrate 93.88% of the cases of highway disasters. Another possible explanation for this is the spread of the social network Twitter as a means of communication for transportation regulatory agencies. 20,611 tweets were published between September 2009 and October 2022, of which 669 were disaster records. Hence, the inventory consists of 303 landslides, 15 rock falls, 76 erosion, 165 floods, 64 road collapses, 16 bridge collapses, and 30 pothole events. The three highways which had the highest number of incidences were BR-101, BR-262, and BR-381 with 111, 79, and 62 disaster events recorded, respectively. Among the states, the highest numbers were recorded in Minas Gerais, with 190 events, Espírito Santo, 114, and Paraná, with 103 incidents. Viana and Serra are highlighted among the flood cases, registering 11 and 8 cases respectively.

The experimental results for HazRoad’s automatic landslide and flood detection are presented in Table 4.

Table 4 – Performance metrics for DL models

Hazard	Batch Size	Learning Rate	Filters	Precision	Recall	F1-Score
Landslide	16	0.0005	4	0.963	0.957	0.960
Flood	8	0.0001	4	0.900	0.923	0.911

Overall, both models show a consistently high level of performance. The F1-score evaluation results for each case demonstrate the applicability of the HazRoad training dataset for disaster detection results. The F1-score for the test dataset on the models ranges from 91% to 96%, which is a good result. Moreover, the same was observed in Precision and Recall models, which range between 90.00%-93.30% and 92.30%-95.70%, respectively. In terms of computational architecture, the landslide detection model proved to need 16 training examples used for each iteration, while the model trained on flood data proved efficient with only 8 iterations. This implies that more computational effort was required to identify mass movements. The results of the hazard prediction by image segmentation are set out in the figure below. On the left are the black and white satellite images. The white polygons represent landslide and flood areas respectively. A closer inspection of Figure 8 shows that despite the high precision values, both models have certain limitations when identifying small areas.

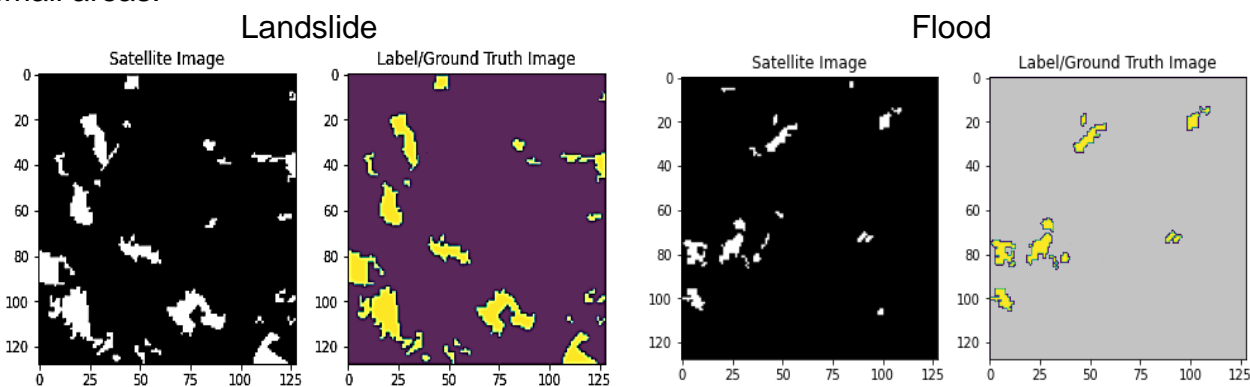


Figure 8 – Hazards predictions

The results of the hazard assessment analysis are set out in Figure 9. Additionally, the weighting of the individual causal hazard factors obtained by the AHP matrix is shown in Table 5.

It can be seen from the maps in the figure below that all sections of the highway in the study area have high vulnerability to hydro-geological disasters. One of the reasons is the geomorphology of the terrain, which presents high altitude, between the region between Viana and Domingos Martins (BR-262) and low altitude mainly in the region of the Municipality of Serra (km's 294,299,300 and 302 of BR-101), an area that tends to flood.

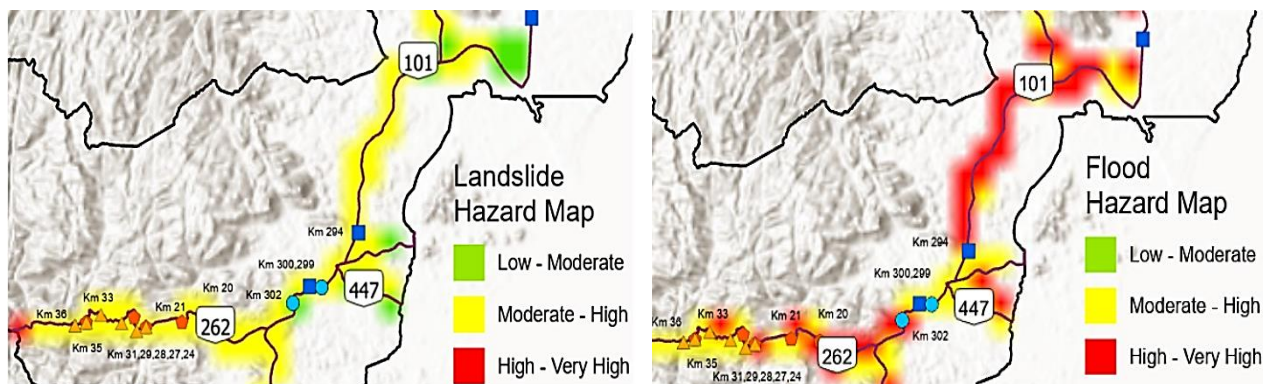


Figure 9 – Hazards maps

It is observed that the instability on slopes increases as the gradient increases, near the Serra, do Caparaó (mountain range west of Km 36 of BR-262). Whereas, areas where the slope angles are below 15° are less susceptible to landslides, in the case of the Serra Municipality. On the other hand, the probability of flooding events rises in the upstream direction of BR-101, in the stretches between Cariacica and Serra.

Table 5 – Hazard Factor Weighting

Hazard	TWI	Elev.	Precip.	Slope	LULC	NDVI	Dist. river	Dist. road	Drainage Density	Soil Type
Landslide	0.202	0.132	0.069	0.230	0.040	0.051	0.047	0.093	0.068	0.068
Flood	0.217	0.200	0.087	0.081	0.056	0.043	0.107	0.047	0.081	0.081

Topography wetness index had the highest impact on the occurrence of floods and landslides. The results suggest a significant accumulation of water across the study area, primarily attributed to the presence of clay soil, which is prevalent in the region. In addition, the hydrological characteristics of the area also contribute to the prevalence of high and very high flood hazard zones. The sections of the highway closest to the Jacu and Vitória rivers experience the most severe impacts in this regard. Concerning the landslide, the areas near the Serra do Caparaó have the higher susceptibility. Because, the region's steep terrain significantly increases the potential for landslides. Furthermore, the geomorphological formation of this area renders it more vulnerable to such events.

4. CONCLUSION

This work contributes to existing knowledge about highway disasters by providing a comprehensive methodology for creating a management system. Web scraping and NLP techniques allow the collection and organization of data for the creation of an inventory. The remote sensing mapping step helps in the rapid delineation of affected areas. Through the use of deep learning image segmentation, new disaster spots can be automatically detected, as the algorithm recognizes impacted areas due to variations in the pixel pattern of the image. The hazard assessment identifies the most disaster-prone areas. Finally, all results are stored in a web portal. It is also interesting to note that the methods used to develop HazRoad can be applied to other roads in other parts of the world.

REFERENCES

1. CNT, National Confederation of Transportation Agency, CNT. Pesquisa de Rodovias CNT (2022). Available: <<https://pesquisarodovias.cnt.org.br/paine/mobile>> (Access date: Mars 2022)
2. DNIT, National Department of Transportation Infrastructure. Anuário Estatístico de Transportes (2020). Available:<https://www.gov.br/infraestrutura/ptbr/assuntos/dadosdetransportes/AnuarioEstatisticodeTranportes2020322_QRcode21.06.2020.pdf> (Access date: April 2022).
3. Agência Senado. Governo federal destina R\$ 200 milhões para recuperar rodovias danificadas por chuvas (2021). Available: <Como fazer referência de site nas normas ABNT em trabalhos acadêmicos – Tecnoblog> (Access date: April 2022).
4. World Road Association, (2022). Disaster Management Manual. Available: <<https://disaster-management.piarc.org/en/preparedness/preparedness-measures>> (Access date: June 2022).
5. Anson, S., Watson, H., Wadhwa, K., & Metz, K. (2017). Analysing social media data for disaster preparedness: Understanding the opportunities and barriers faced by humanitarian actors. *International Journal of Disaster Risk Reduction*, 21, 131–139. <https://doi.org/10.1016/j.ijdr.2016.11.014>
6. Joyce, K. E., Belliss, S. E., Samsonov, S. V., McNeill, S. J., & Glassey, P. J. (2009). A review of the status of satellite remote sensing and image processing techniques for mapping natural hazards and disasters. *Progress in Physical Geography: Earth and Environment*, 33(2), 183–207.
7. Yu, M.; Yang, C.; Li, Y. Big Data in Natural Disaster Management: A Review. *Geosciences* (2018). Vol 8, pp 165. <https://doi.org/10.3390/geosciences8050165>
8. Peng, B.; Meng, Z.; Huang, Q.; Wang C. (2019). Patch Similarity Convolutional Neural Network for Urban Flood Extent Mapping Using Bi-Temporal Satellite Multispectral Imagery. *Remote Sensing* 11, no. 21: 2492. <https://doi.org/10.3390/rs11212492>
9. Liu Z, Gilbert G. Cepeda J. M., Lysdahl A. O. K., Piciullo L., Hefre H. Lacasse S., (2021) Modelling of shallow landslides with machine learning algorithms, *Geoscience Frontiers*, Volume 12, Issue1, 2021, Pages 385-393, ISSN 1674-9871. <https://doi.org/10.1016/j.gsf.2020.04.014>.
10. Roberto Bentivoglio R., Isufi E., Nicolaas J. S., Taormina R., (2022). Deep Learning Methods for Flood Mapping: A Review of Existing Applications and Future Research Directions <https://doi.org/10.5194/hess-2022-83> Preprint. Discussion started: 2 March 2022 [hess-2022-83.pdf](https://doi.org/10.5194/hess-2022-83) (copernicus.org)
11. CEMADEN, Centro Nacional de Monitoramento de Alertas de Desastres Naturais (2017). Apresentação. Available: < <http://www2.cemaden.gov.br/apresentacao/> > (Access date: July 2022)
12. Maldonado M., Alulema D., Morocho D., Proano M., (2016). System for monitoring natural disasters using natural language processing in the social network Twitter. 1-6. 10.1109/CCST.2016.7815686.
13. Hernandez-Suarez, A.; Sanchez-Perez, G.; Toscano-Medina, K.; Perez-Meana, H.; Portillo-Portillo, J.; Sanchez, V.; García Villalba, L.J., (2019). Using Twitter Data to Monitor Natural Disaster Social Dynamics: A Recurrent Neural Network Approach with Word Embeddings and Kernel Density Estimation *Sensors* 2019, 19, 1746. <https://doi.org/10.3390/s19071746>
14. Setiawan Y., Gunawan D., and Efendi R., "Feature Extraction TF-IDF to Perform Cyberbullying Text Classification: A Literature Review and Future Research Direction, (2022). *International Conference on Information Technology Systems and Innovation (ICITSI)*, Bandung, Indonesia, 2022, pp. 283-288, doi: 10.1109/ICITSI56531.2022.9970942.
15. Géron A., (2019). *Hands-On Machine Learning with Scikit-Learn, Keras, and TensorFlow*, 2nd Released September 2019 Publisher(s): O'Reilly Media, Inc. ISBN: 9781492032649
16. Alpaydin, E., (2014) *Introduction to machine learning / Ethem Alpaydin—3rd ed. p. cm. Includes bibliographical references and index.* ISBN 978-0-262-02818-9 (hardcover: alk. paper) 1. Machine learning. I. Title Q325.5.A46 2014 006.3'1—dc23
17. IBM, (2022). What is Deep Learning? | IBM. Available: <<https://www.ibm.com/topics/deep-learning>> (Access date: August 2022).
18. Luz, K.; Tavares, J.E.D.R.; Barbosa, J.L.V.; Iglesia, D.H.D.L.; Leithardt, V.R.Q., (2021). RoadLytics: Road Accidents Analytics Using Artificial Intelligence to Support Deaths Prevention on Highways. *Preprints* 2021, 2021050698. <https://doi.org/10.20944/preprints202105.0698.v1>.
19. Tin Kam, H., (1995). Random decision forests. In *Proceedings of the 3rd International Conference on Document Analysis and Recognition*, Montreal, QC, Canada, 14–16 August 1995; Volume 1, pp. 278–282.
20. Cortes, C., Vapnik, V., (1995). Support-vector networks. *Mach. Learn.* 1995, 20, 273–297. *Support-vector networks | SpringerLink*
21. Ronneberger, O., Fischer, P., & Brox, T. (2015). U-Net: Convolutional Networks for Biomedical Image Segmentation (pp. 234–241). https://doi.org/10.1007/978-3-319-24574-4_28
22. Mseddi, W.S.; Ghali, R.; Jmal, M.; Attia, R., (2021). Fire Detection and Segmentation using YOLOv5 and U-NET. In *Proceedings of the 29th European Signal Processing Conference (EUSIPCO)*, Dublin, Ireland, 23–27 August 2021; pp. 741–745.

23. Meena, S. R., Nava, L., Bhuyan, K., Puliero, S., Soares, L. P., Dias, H. C., Floris, M., and Catani, F.,(2022): HR-GLDD: A globally distributed dataset using generalized DL for rapid landslide mapping on HR satellite imagery, *Earth Syst. Sci. Data Discuss.* [preprint], <https://doi.org/10.5194/essd-2022-350>, in review, 2022.
24. Filipponi, F., (2019). Sentinel-1 GRD Preprocessing Workflow. *Proceedings 2019*, 18, 11. <https://doi.org/10.3390/ECRS-3-06201>
25. Corbane C., Politis P., Kempeneers P., Simonetti D., Soille P., Burger A., Pesaresi M., Sabo F., Syrris V., Kemper T.,(2020).A global cloud-free pixel-based image composite from Sentinel-2 data. *Data in Brief*, Vol 31, 2020,105737, ISSN 2352-3409. <https://doi.org/10.1016/j.dib.2020.105737>.
26. Griffiths P., van der Linden S., Kuemmerle T., Hostert P., (2013). A Pixel-Based Landsat Compositing Algorithm for Large Area Land Cover Mapping, *IEEE J. Sel. Top. Appl. Earth Obs. Remote Sens.* 6 (2013) 2088–2101 <https://doi.org/10.1109/JSTARS.2012.2228167>.
27. White J. C., Wulder M. A., Hobart G. W, Luther J. E., Hermosilla T., Griffiths P., Coops N. C., Hall R. J., Hostert P., Dyk A., Guindon L. (2014). Pixel-Based Image Compositing for Large-Area Dense Time Series Applications and Science, *Canadian Journal of Remote Sensing*, 40:3, 192-212, DOI:10.1080/07038992.2014.945827
28. Scheip, C. M., Wegmann, K. W.: HazMapper, (2021): a global open-source natural hazard mapping application in Google Earth Engine, *Nat. Hazards Earth Syst. Sci.*, Vol 21, pp 1495–1511. <https://doi.org/10.5194/nhess-21-1495-2021>.
29. UNDRR, United Nations Office for Disaster Risk Reduction Hazard Terminology. Available:< <https://www.undrr.org/terminology/hazard> >. (Access date: November 2022)
30. Solheim, A., R. Bhasin, F. V. D. Blasio, L. H. Blikra, S. Boyle, A. Braathen, J. Dehls, (2005). "International Centre for Geohazards (ICG): Assessment, Prevention, and Mitigation of Geohazards." *Norwegian Journal of Geology* 85: 45–62.
31. The World Bank, (2019). "Road Geohazard Risk Management Handbook." World Bank, Washington, DC. License: Creative Commons Attribution CC BY 3.0 IGO
32. Antzoulatos, G.; Kouloglou, I.; Bakratsas, M.; Moutzidou A.; Gialampoukidis, I.; Karakostas, (2022). A.; Lombardo, F.; Fiorin, R.; Norbiato, D.; Ferri, M.; et al. Flood Hazard and Risk Mapping by Applying an Explainable Machine Learning Framework Using Satellite Imagery and GIS Data. *Sustainability* 2022, 14, 3251. <https://doi.org/10.3390/su14063251>
33. Farr, T. G., et al. (2007), The Shuttle Radar Topography Mission, doi:10.1029/2005RG000183.
34. SRTM, NASA Shuttle Radar Topography Mission (SRTM) (2013). Shuttle Radar Topography Mission Global. Distributed by Open Topography. <https://doi.org/10.5069/G9445JDF>. (Access date: July 2022)
35. IJSN, Instituto Jones dos Santos Neves, (2012). Sartório, J. L., Nascimento, T. M., Vieira R. D. S. Mapeamento geomorfológico do estado do Espírito Santo. Vitória, ES.
36. ANA, Agência Nacional de Águas e Saneamento Básico (2021)- Organizações - Portal de Dados Abertos da Available: < <https://dados.ana.gov.br/organization/ana> > (Access date: December 2022).
37. G1 ES, (2022). BR-262 tem novo deslizamento na região Serrana do ES. Available:< <https://g1.globo.com/es/espírito-santo/noticia/2019/11/19/br-262-tem-novo-deslizamento-na-regiao-serrana-do-es.ghtml>> (Access date: December 2022).
38. Yang W., Wang M., and Shi P., (2013)."Using MODIS NDVI Time Series to Identify Geographic Patterns of Landslides in Vegetated Regions," in *IEEE Geoscience and Remote Sensing Letters*, vol. 10, no. 4, pp. 707-710, doi: 10.1109/LGRS.2012.2219576.
39. Zhu Z., Woodcock C.E, (2014). Continuous change detection and classification of land cover using all available Landsat data, *Remote Sensing of Environment*, Vol 144, pp 152-171,ISSN 0034-4257, <https://doi.org/10.1016/j.rse.2014.01.011>
40. EOS Data Analytics (2023). NDVI Mapping in Agriculture, Index Formula, And Uses. Available:<<https://eos.com/make-an-analysis/ndvi/>> (Access date: January 2023)
41. Gessesse A. A., Melesse, A. M, (2019). Temporal relationships between time series CHIRPS-rainfall estimation and eMODIS-NDVI satellite images in Amhara Region, Ethiopia. *Hydrology and Climate Variability*. Elsevier, pp 81-92, ISBN 9780128159989 7.
42. CEPEDEC, Coordenadoria Estadual de Proteção e Defesa Civil (2020). Available:< <https://cb.es.gov.br/Media/CBMES/PDF's/Release%2002-03-2020%20-%2011h.pdf>> (Access date: December 2022).
43. Saaty, T. L. (1988). What is the analytic hierarchy process? Springer Berlin Heidelberg, pp. 109-121.
44. Kayastha P., Dhital M.R, De Smedt F.,Application of the analytical hierarchy process (AHP) for landslide susceptibility mapping: A case study from the Tinau watershed, west Nepal, (2013). *Computers & Geosciences*, Vol.52, 2013, pp 398-408, ISSN 0098-3004, <https://doi.org/10.1016/j.cageo.2012.11.003>.
45. Danumah, J.H., Odai, S.N., Saley, B.M.et al. (2016). Flood risk assessment and mapping in Abidjan district using multi-criteria analysis (AHP) model and geoinformation techniques, (cote d'ivoire). *Geoenvon Disasters*.Vol 3, pp10. <https://doi.org/10.1186/s40677-016-0044-y>
46. Panchal, S., & Shrivastava, A. K. (2022). Landslide hazard assessment using analytic hierarchy process (AHP): A case study of National Highway 5 in India. *Ain Shams Engineering Journal*, 13(3), 101626.